Biochemical and Biophysical Research Communications 441 (2013) 1011–1017

Contents lists available at ScienceDirect

Biochemical and Biophysical Research Communications

journal homepage: www.elsevier.com/locate/ybbrc

Construction and characterization of functional anti-epiregulin humanized monoclonal antibodies

Young-Hun Lee [a,b], Mariko Iijima [a], Yuji Kado [c], Eiichi Mizohata [c], Tsuyoshi Inoue [c], Akira Sugiyama [a], Hirofumi Doi [a,*], Yoshikazu Shibasaki [a,*], Tatsuhiko Kodama [a]

[a] Laboratory for Systems Biology and Medicine, Research Center for Advanced Science and Technology, The University of Tokyo, 4-6-1 Komaba, Meguro-ku, Tokyo 153-8904, Japan
[b] Department of Life Sciences, Graduate School of Arts and Sciences, The University of Tokyo, 3-8-1 Komaba, Meguro-ku, Tokyo 153-8902, Japan
[c] Department of Applied Chemistry, Graduate School of Engineering, Osaka University, 2-1 Yamadaoka, Suita, Osaka 565-0871, Japan

ARTICLE INFO

Article history:
Received 25 October 2013
Available online 12 November 2013

Keywords:
Epiregulin
Humanization
Antibody engineering
Resurfacing
Antibody-dependent cellular cytotoxicity

ABSTRACT

Growth factors are implicated in several processes essential for cancer progression. Specifically, epidermal growth factor (EGF) family members, including epiregulin (EREG), are important prognostic factors in many epithelial cancers, and treatments targeting these molecules have recently become available. Here, we constructed and expressed humanized anti-EREG antibodies by variable domain resurfacing based on the three-dimensional (3D) structure of the Fv fragment. However, the initial humanized antibody (HM0) had significantly decreased antigen-binding affinity. Molecular modeling results suggested that framework region (FR) residues latently important to antigen binding included residue 49 of the light chain variable region (VL). Back mutation of the VL49 residue (tyrosine to histidine) generated the humanized version HM1, which completely restored the binding affinity of its murine counterpart. Importantly, only one mutation in the framework may be necessary to recover the binding capability of a humanized antibody. Our data support that HM1 exerts potent antibody-dependent cellular cytotoxicity (ADCC). Hence, this antibody may have potential for further development as a candidate therapeutic agent and research tool.

1. Introduction

The epidermal growth factor (EGF) signaling system consists of at least seven ligands, that is, EGF, amphiregulin, transforming growth factor α, heparin-binding EGF, betacellulin, epiregulin (EREG), and epigen [1]. These ligands bind to the extracellular region of the EGF receptor (EGFR) and induce a conformational change in EGFR, leading to its dimerization and activation. Subsequently, activated EGFR stimulates many intracellular signaling pathways, such as the mitogen-activated protein kinase (MAPK) and phosphoinositide 3-kinase (PI3K)/Akt pathways, and promotes proliferation, cell survival, and angiogenesis [1,2]. In many different cancer cells, EGFR ligands are produced either by the cancer cells themselves or by surrounding stromal cells, leading to constitutive EGFR activation [3]. Of the EGF ligands, EREG is produced as a transmembrane precursor and exerts mitotic activity in various primary cell types, such as rat hepatocytes, and various types of human cancer cells, particularly epithelial tumor cells [4,5]. Interestingly, EREG is expressed at relatively low levels in most adult normal tissues, but is highly expressed in various human cancers, including colon, breast, prostate, and ovary cancers [6–9]. Many studies have demonstrated the possible involvement of EREG in tumorigenesis and the oncogenic effects of cancer-specific overexpression of EREG. Thus, EREG is likely to be involved in the development of a variety of human cancers, and its potential use as a therapeutic target is being intensely investigated. To this end, several anti-EREG murine monoclonal antibodies (mAbs) have been successfully tested *in vivo* (unpublished data). However, one of the primary problems in developing monoclonal antibodies as drugs is the human anti-mouse antibody response (HAMA), which limits the administration of murine antibodies [10]. In this study, we have described the construction and expression of humanized anti-EREG antibodies with high-affinity targeted cytotoxicity and decreased immunogenicity through resurfacing the variable region and recombination.

2. Materials and methods

2.1. Materials

9E5, a human anti-EREG antibody, was a member of a panel of murine monoclonal antibodies (mAbs) generated using a subtractive immunization protocol in hybridoma cells and was provided

* Corresponding authors. Fax: +81 3 5452 5232.
E-mail addresses: doi-h@lsbm.org (H. Doi), shibasaki@lsbm.org (Y. Shibasaki).

0006-291X/$ - see front matter © 2013 Elsevier Inc. All rights reserved.
http://dx.doi.org/10.1016/j.bbrc.2013.11.014

as a kind gift by Dr. Kenji Yoshida (Forerunner Pharma Research, Tokyo, Japan), along with its sequence information. The nucleotide sequences of 9E5 heavy and light variable regions (VH and VL, respectively), synthesized by Hokkaido System Science (Sapporo, Japan), were inserted into the pUC57 vector.

2.2. Modeling the variable fragment (Fv) of 9E5

The 3D structure of the 9E5 variable region was constructed by homology modeling based on Ig VH and VL domains with highly matched amino acid sequences and known structures. The Protein Data Bank (PDB) was searched for antibody sequences with more than 70% similarity to the 9E5 variable region. Two separate BLASTP searches were performed for VH and VL. Candidate template structures were selected based on the IMGT database for residue numbering and CDR location [11]. For refining the modeling of the CDR conformations, CDR loop template structures were selected based on the framework region sequence identity of two sides of the CDR loop and the canonical structure type of the CDR loop in candidate template structures. Canonical structures were used to predict the backbone structures of CDRs L1–3, H1, and H2 [12]. Only CDR H3 and the neighboring side chains were remodeled de novo using a kinematic loop modeling algorithm in a Rosetta protocol. The complex models of 9E5 VH and VL were built with Rosetta Antibody [13]. The 200 lowest energy conformations from this run were extracted and subjected to energy minimization. The five lowest energy conformers were used in subsequent analyses. Differences between murine and humanized variants of HM0 antibodies were individually analyzed to investigate their possible influence on the CDRs.

2.3. Humanization of 9E5 antibodies

We chose human variable regions that were the most homologous in sequence to the murine variable regions as the human framework for humanized 9E5 antibodies. 9E5 VH and VL sequences were subjected to separate IgBLAST searches against the immunoglobulin GenBank database. A set of human data, which contained 1000 antibody sequences sharing the highest identities with 9E5, was selected for each variable region, and another set of murine data was chosen in the same way. Several systematic differences were found when comparing the murine and human selections, and these were collected as candidates for humanization, excluding the CDR residues. Candidates from differential regions were selected according to the analysis of the constructed model and the following criteria: (i) the candidates were located within the solvent accessible surface area according to CHIMERA [14]; (ii) surface residues of 9E5 variable regions (defined as having >30% relative solvent accessibility) [15] were found by aligning the sequences of antibodies of known structure to the sequence of 9E5 to identify homologous positions; (iii) the candidates could not form pivotal contacts comprising intermolecular hydrogen bonds between VH and VL or intramolecular hydrogen bonds that were important for retaining the conformation of CDRs and interaction with CDRs directly; and (iv) the candidates were only differential residues, not unique residues.

2.4. Construction, expression, and purification of antibodies

Humanized VH and VL gene sequences were subcloned into predigested expression vectors containing the human interleukin 2 (IL2) signal sequence [16] and encoding human IgG1, including the constant hinge, CH2, and CH3 regions. Humanized anti-EREG heavy and light chain expression plasmids were cotransfected into CHO-S host cells. Selection of cell lines was followed by puromycin selection (5–15 μg/mL) to obtain high and stable expression of humanized mAbs. Conditioned media containing humanized mAbs was harvested and passed through a 0.2-μm filter. The clarified supernatant was purified using Bio-Scale Mini UNOsphere SUPrA (Bio-Rad, Hercules, CA, USA) according to the manufacturer's recommendations. Eluted antibodies were neutralized with 1 M Tris–HCl (pH 9), and buffer exchange was carried out using phosphate-buffered saline (PBS) through dialysis of purified antibodies overnight. The concentration of the purified antibodies was determined by measuring the absorbance at 280 nm.

2.5. Cell lines and culture

Human colonic adenocarcinoma cell lines, including HCT116 (American Type Culture Collection [ATCC], CCL-247) and DLD-1 (ATCC, CCL-221), and a human gastric cancer cell line, AGS (ATCC, CRL-1739), were propagated and maintained according to the manufacturer's instructions.

2.6. Immunostaining

Cells were cultured on cover glass and fixed with ice-cold ethanol for 10 min. After three washes with PBS, nonspecific sites were blocked with 1 × PBS and 0.2% fish skin gelatin (PBS/FSG) for 10 min. The primary antibodies (9E5, HM0, and HM1) were diluted to 0.1 mg/mL in PBS/FSG, 50 μL of diluted primary antibodies was added to each well, and coverslips were incubated at room temperature (RT) for 1 h. Following three washes with PBS/FSG, the samples were incubated for 30 min with appropriate secondary antibodies (Alexa Fluor 488-labeled mouse/human anti-IgG). Images were taken using a Leica DM LB microscope (Leica Microsystems).

2.7. Flow cytometry

Cells were detached from culture plates with PBS containing 2 mM EDTA at RT for 10–20 min and centrifuged at 1000 rpm for 5 min. Detached cells were washed once with PBS and were then resuspended in FACS buffer (PBS containing 1% bovine serum albumin [BSA], 0.1 mM EDTA, and 0.01% NaN_3). The cells were counted, plated at 1×10^5 cells per well in 96-well plates (50 μL volume per well), and kept on ice for 30 min. After washing three times with ice-cold FACS buffer, the cells were then incubated in the presence or absence of 0.1, 0.5, or 1 μg/mL Alexa Fluor 488-labeled antibodies in 10 μL of ice-cold FACS buffer. After 1 h of incubation on ice in the dark, cells were washed three times with ice-cold FACS buffer. Subsequently, cells were resuspended in 200 μL FACS buffer and analyzed by Guava EasyCyte (Millipore). The experiment was performed in triplicate, and data were analyzed with GuavaSuite (Millipore).

2.8. Surface plasmon resonance (SPR)

SPR measurements were performed on a Biacore T200 instrument (GE Health Sciences). Antibodies were immobilized onto a CM5 chip using standard amine-coupling chemistry addressing flow cells individually (200 RU level). Human EREG-Fc (MW, 76 kDa), used as a ligand for antibodies, was serial diluted into HBS-EP + buffer (GE Health Sciences) to obtain 1.5 μM, 300, 60, 12, and 2.4 nM concentrations. Each hEpiregulin-Fc was titrated from low to high concentration samples, and single-cycle kinetic analysis was performed with an on-time of 120 s and an off-time of 600 s at 30 μL/min. Curve fitting and K_D determinations were performed with the Biacore T200 Evaluation software and were used to evaluate the data assuming a bivalent analyte model. The results were based on three independent experiment repeats.

2.9. ADCC assay

ADCC assays were performed using Jurkat NFAT luciferase reporter cells (Promega, Madison, WI, USA), that is, effector cells that stably express the FcγRIIIa receptor, V158 variant, and an NFAT-response element driving expression of firefly luciferase. Target cells (2×10^4/well) prepared in ADCC assay buffer (RPMI 1640 medium with 4% low IgG serum supplemented with 100 IU/mL penicillin and streptomycin) were added to each well. Serial dilutions of antibodies (threefold dilutions from 2000 to 0.3 ng/mL) were added and incubated for 2 h at 37 °C with 5% CO_2. After two washes with ADCC assay buffer, Jurkat NFAT luciferase reporter cells were added to each well, for a 5:1 effector:target cell ratio, and the plates were incubated for an additional 24 h. Bio-Glo luciferase assay reagent (Promega) was then added to each well, and the plates were incubates at RT for 10 min, followed by luminescence measurements on a plate reader.

3. Results

3.1. 3D structure modeling of 9E5 antibodies

For the variable region of 9E5, the top 20 sequences were identified according to framework region (FR) identity, which was defined as greater than 70% sequence identity. A global alignment was manually constructed by adjusting for differences in the CDRs, and a first ranking was performed based on sequence identity (excluding CDRs). For 9E5 VH and VL, 10 and 4 sequences, respectively, were found to have more than 90% FR identity. The crystallographic resolution and sources of the top 10 selected variable domain sequences for 9E5 VH and the VL were assessed (Supplementary Table 1). The antibody 3T3P (PDB codes) showed 95% FR identity with the 9E5 VH, while 2ADF (PDB codes) showed 98% FR identity with the 9E5 VL. Moreover, the CDRs of the light chains (L1, L2, and L3) of 2ADF (86–100% sequence identity) were very similar to 9E5, and CDRs 1 and 2 of the heavy chain of 9E5 templates, i.e., 1J05 (100% sequence identity) and 3Q3G (94% sequence identity), were chosen for H1 and H2, respectively. All CDRs other than H3 were modeled using templates in the PDB, whereas CDR-H3 was remodeled de novo using a kinematic loop modeling algorithm in a Rosetta protocol [17]. After homology modeling, the best discrete optimized protein energy score result was optimized to establish the final 3D model of 9E5 using energy minimization (Fig. 1A). Recently, the crystal structure of 9E5 in apo-form and complexed with its antigen was resolved (Kado et al., manuscript in preparation); the similarities between the crystal structure and the modeled structure will be discussed in a separate report.

3.2. Humanization of 9E5 antibodies

Using the modeled 9E5, we identified residues that should be mutated to obtain HM0. Moreover, a human target sequence homologous to 9E5 variable regions was identified by searching the immunoglobulin GenBank database. By combining information on which positions were surface exposed with an alignment of the most homologous human variable region sequence, surface positions of 9E5 displaying nonhuman residues were identified (Fig. 1A). Fourteen of the nonhuman residues in HM0-VH were surface residues, and 13 of the nonhuman residues in HM0-VL were exposed residues (Fig. 1B). Within these candidates, five residues (H1Q, H12K, H23K, H40A, and H82E) in VH and five residues (L17D, L42Q, L49Y, L69T, and L79Q) in VL were mutated; these changes would affect the charge of the antibody (amino acids are identified by their chain, H or L, the single-letter amino acid code, and their position in the sequence). Other candidates with differential residues were considered; for these, the structures of side chains would become smaller, but the physical and chemical characteristics related to charge, hydrophobicity, and polarity would be similar.

However, our results indicated that the initial version of the humanized antibody (HM0) lost its binding activity (Table 1), which may have resulted from mutations near the antigen-binding site causing loss of binding affinity. Thus, we sought to identify mutated residues that played an important part in constructing the CDR loops upon mutation to their respective human consensus sequence. Of these, six FR residues (H23K, H38R, H48M, H97A, L33L, and L49Y), which were near the CDRs (within ~5 Å), were identified. Additional modeling revealed that residue L49Y produced some rearrangements of the neighboring side chains and possibly modified the overall conformation of the CDR-L2 loop (Supplementary Fig. 1). Other FR residues produced either stabilized the conformation of CDR loops or did not bind to EREG. Therefore, L49Y was 'back-mutated' into the first humanized construct to obtain the HM1 antibody.

3.3. Production of anti-EREG antibodies

Anti-EREG mAbs were purified by protein A agarose-affinity chromatography and analyzed by SDS–PAGE under reducing conditions. Two polypeptides of approximately 55 and 25 kDa, corresponding to the heavy and light chains, respectively, were identified. The cell lines synthesizing these proteins secreted intact human IgG1 with yields from 4 to 10 μg/mL/10^6 cells (data not shown).

3.4. Binding activity of antibodies to EREG expressed on the cell surface and other subcellular locations

To elucidate the binding activity of each antibody, we examined the cell surface and subcellular localization of EREG by immunofluorescence staining. For this purpose, antibody-binding assays were performed using colorectal carcinoma cells (DLD-1, HCT116) and gastric cancer cells (AGS). 9E5 and HM1 were detected predominantly as intense green florescence spots in the cell surface with some faint fluorescence demonstrating subcellular distribution in colon cancer cells (Fig. 2A). HM0 also exhibited weak and diffuse cell surface stained (Fig. 2A). This confirmed the antibody-binding activity and accumulation of EREG on the cell surface in colon cancer cells. Binding assays in gastric cancer cells supported the low expression of EREG in these cells, and no antibody binding was observed (data not shown). We further analyzed the subcellular localization of EREG under permeabilization conditions.

3.5. Binding efficiency of anti-EREG antibodies by flow cytometry

The cell surface binding efficiency of each antibody to EREG-expressing cells was determined by flow cytometry as described in Section 2. DLD-1 and HCT116 cells were used as $EREG^+$ cells, and AGS cells were used as a negative control. In these assays, binding efficiency was tested by adding various concentrations (0–1 μg/mL) of each antibody to cells, followed by staining with Alexa Fluor 488-labeled antibodies. The results of flow cytometry indicated that HM1 bound more efficiently to DLD-1 and HCT116 cells than the same concentration of HM0 (Fig. 2B). The binding efficiency was found to be dependent on the concentration of the antibody used. Importantly, HM1 was able to bind EREG-expressing cells at a relatively low concentration (0.1 μg/mL), while HM0 was not.

3.6. Binding affinity determination

Interactions between EREG and each antibody were compared by real-time SPR analyses. Next, we measured the binding affinity and kinetics of human EREG-Fc (analytes) to each antibody coupled as ligand to a CM5 sensor chip. Initially, we tested several potential regeneration conditions (acidic, high salt, addition of chelator or detergent) for incomplete removal of human EREG-Fc

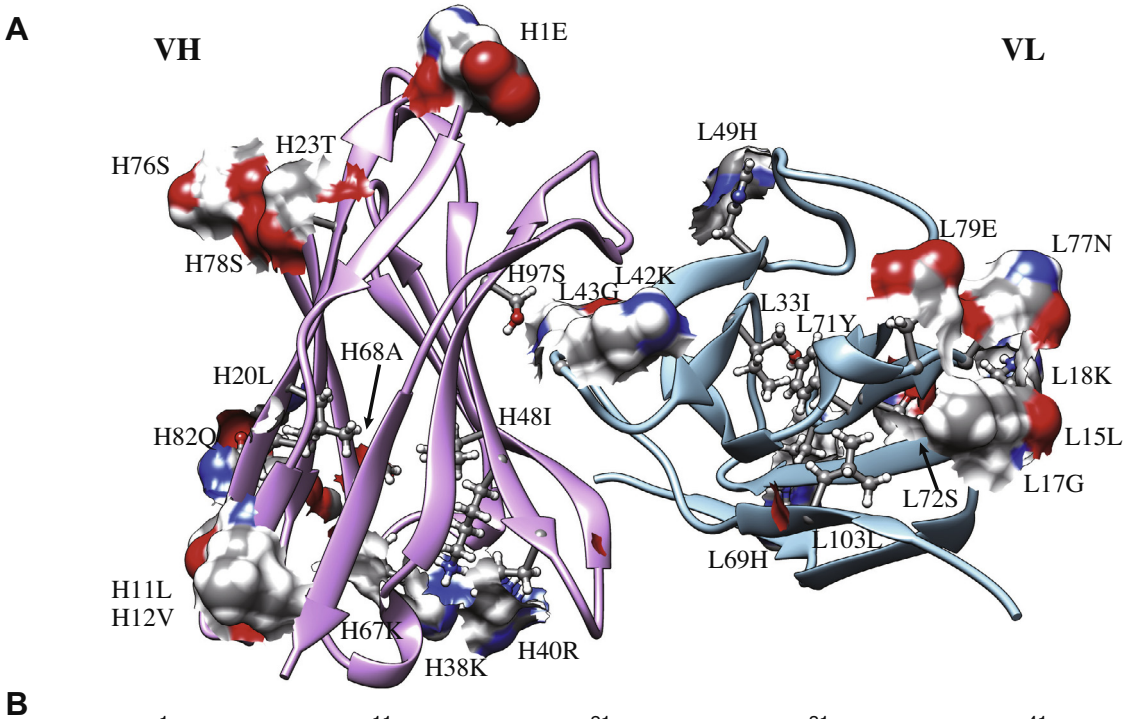

B

```
                1                   11                  21                  31                  41
Conservation
Charge variation
9E5_VH      EVQLQQSGAE  LVKPGASVKL  SCTASGFNIK  DTYMHWVKQR  PEQGLEWIGR
HM0_VH      QVQLQQSGAE  VKKPGASVKV  SCKASGFNIK  DTYMHWVRQA  PEQGLEWMGR
HM1_VH      QVQLQQSGAE  VKKPGASVKV  SCKASGFNIK  DTYMHWVRQA  PEQGLEWMGR

               51                  61                  71                  81                  91
Conservation
Charge variation
9E5_VH      IDPLNDKTKY  DPKFQGKATI  TADTSSNSAY  LQLSSLTSED  TAVYYCSRGG
HM0_VH      IDPLNDKTKY  DPKFQGRVTI  TADTSTNTAY  LELSSLTSED  TAVYYCARGG
HM1_VH      IDPLNDKTKY  DPKFQGRVTI  TADTSTNTAY  LELSSLTSED  TAVYYCARGG

              101                 111
Conservation
Charge variation
9E5_VH      GDPVFVYWGQ  GTLVTVSA
HM0_VH      GDPVFVYWGQ  GTLVTVSA
HM1_VH      GDPVFVYWGQ  GTLVTVSA

                1                   11                  21                  31                  41
Conservation
Charge variation
9E5_VL      DIQMTQSPSS  LSASLGGKVT  ITCKASQDIN  KYIAWYQHKP  GKGPRLLIHY
HM0_VL      DIQMTQSPSS  LSASVGDRVT  ITCKASQDIN  KYLAWYQHKP  GQAPRLLIYY
HM1_VL      DIQMTQSPSS  LSASVGDRVT  ITCKASQDIN  KYLAWYQHKP  GQAPRLLIHY

               51                  61                  71                  81                  91
Conservation
Charge variation
9E5_VL      TSTLHPGIPS  RFSGSGSGRD  YSFSISNLEP  EDIATYYCLQ  YDNLRTFGGG
HM0_VL      TSTLHPGIPS  RFSGSGSGTD  FTFSISSLQP  EDIATYYCLQ  YDNLRTFGGG
HM1_VL      TSTLHPGIPS  RFSGSGSGTD  FTFSISSLQP  EDIATYYCLQ  YDNLRTFGGG

              101
Conservation
Charge variation
9E5_VL      TKLEIKRT
HM0_VL      TKVEIKRT
HM1_VL      TKVEIKRT
```

Fig. 1. (A) View of the 9E5 variable region constructed by homology modeling. (B) Amino acid sequences of anti-epiregulin antibody heavy and light chain variable regions. The CDRs are enclosed with red brackets. Identical residues between the mouse and human consensus sequences are marked in grey, and differing residues are marked in blue (charge variation) or green (non-charge variation). The residues that were reconstituted during humanization are indicated in red.

Table 1
Kinetic parameters for anti-EREG antibodies. All parameters were determined by Biacore analysis and are expressed as mean ± SD values.

Antibody	K_{a1}(1/Ms)	K_{a2}(1/Rus)	K_{d1}(1/s)	K_{d2}(1/s)	K_D(M)
9E5	$3.42 \pm 1.04 \times 10^{5}$	$2.45 \pm 0.16 \times 10^{-3}$	$4.07 \pm 2.11 \times 10^{-3}$	$3.62 \pm 0.57 \times 10^{-2}$	$3.68 \pm 0.63 \times 10^{-8}$
HM0	$6.12 \pm 1.70 \times 10^{4}$	$3.37 \pm 0.86 \times 10^{-6}$	$5.30 \pm 1.02 \times 10^{-3}$	$7.16 \pm 0.26 \times 10^{-4}$	$8.33 \pm 1.45 \times 10^{-7}$
HM1	$2.98 \pm 1.40 \times 10^{5}$	$2.52 \pm 0.19 \times 10^{-3}$	$3.47 \pm 3.43 \times 10^{-3}$	$3.19 \pm 0.76 \times 10^{-2}$	$4.53 \pm 0.89 \times 10^{-8}$

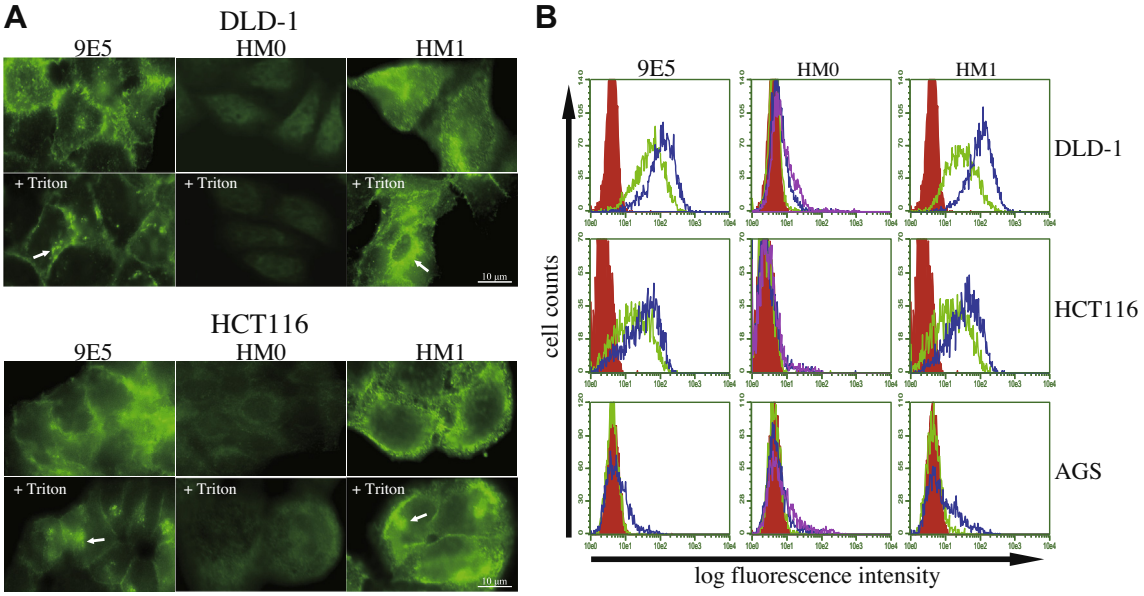

Fig. 2. (A) Immunofluorescent staining of antibodies in human colorectal carcinoma cells. DLD-1 and HCT116 cells, representing two human colorectal carcinoma cell lines, were fixed with paraformaldehyde and treated with or without 0.2% Triton X-100 solution (localization to endomembranes was observed; white arrow). (B) Flow cytometry analysis. Antibodies were tested for their ability bind to the surface of each cell line (DLD-1, HCT116, and AGS). Green line: 0.1 μg/mL, blue line: 0.5 μg/mL, purple line: 1 μg/mL, red line: negative control (0 μg/mL). Data are representative of three independent experiments, all with similar results.

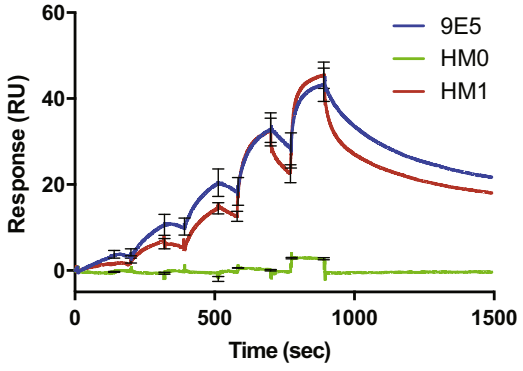

Fig. 3. Single-cycle kinetic analysis of 9E5, HM0, and HM1 antibody binding to an amine-coupled CM5 chip on Biacore. hEpiregulin-Fc was injected at concentrations of 1.5 μM, 300, 60, 12, and 2.4 nM, respectively, and analyzed in duplicate binding cycles over three differing capacity reaction surfaces.

from the biosensor with immobilization of each antibody. In addition, reduced antibody activity was observed in subsequent measurements for all cases (data not shown). Therefore, all Biacore data reported in this study were obtained from single-cycle kinetic experiments. In single-cycle mode, the analyte is injected in increasing concentrations within a single scan and without surface regeneration between injections. Importantly, both modes provide very similar kinetic rate constants [18]. Fig. 3 shows the experimental sensorgrams obtained. The kinetic rate constants (k_{a1}, k_{a2}, k_{d1}, and k_{d2}), as well as equilibrium dissociation constant (K_D), were estimated by global fitting analysis of the titration curves to the bivalent analyte model. The results of this analysis are summarized in Table 1. Good fitting of experimental data to the calculated curves was observed, suggesting the correctness of the fitting model used. Generally, HM1 had slower off rates than HM0. Additionally, HM1 had a lower apparent K_D (20-fold lower) than HM0, and HM1 and 9E5 showed binding kinetics similar to that of human EREG-Fc, with binding affinities of 45 and 37 nM, respectively.

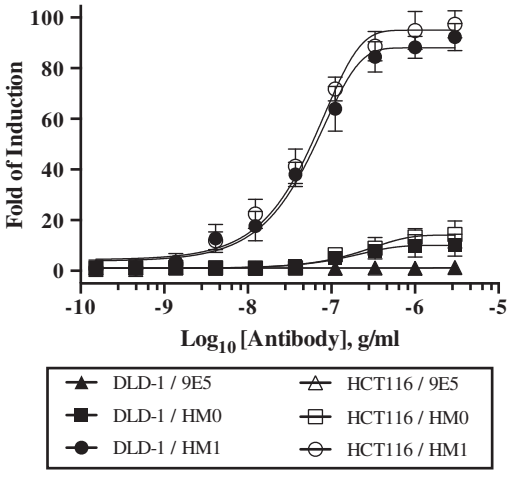

Fig. 4. Anti-epiregulin antibodies induced NFAT-driven luciferase activity in Jurkat cells expressing human FcγRIIIa. Data were fitted using the 4PLC curve fit of the GraphPad Prism software.

3.7. ADCC assay

ADCC function is important for the *in vivo* activity of many therapeutic mAbs. Thus, we assessed the ADCC activity using Jurkat NFAT luciferase reporter cells as described in Section 2. The cellular cytotoxicity of each antibody to colon cancer cells (DLD-1 and HCT116 cells) with enhanced FcγRIIIa binding was evaluated (Fig. 4). Consequently, we generated humanized anti-EREG mAbs (HM1) and examined their effector properties. Analysis of the ADCC in DLD-1 cells revealed that HM1 possessed the highest levels of cellular cytotoxicity, exhibiting a 90-fold increase in cytotoxicity ([induced − background]/[no antibody control − background]) at a concentration of 2 μg/mL, whereas HM0 induced only a 10-fold increase in cytotoxicity when used at the same concentration. However, no significant differences in the ADCCs of 9E5 in colon cancer cells were found with varying concentrations. The results of the ADCC assay for the 9E5 antibody were inconsistent with those obtained in binding assays.

4. Discussion

Cancer therapy has undergone a major revolution characterized by the introduction of targeted drugs that inhibit specific molecules. In the past decade, researchers have begun to recognize that the EGF family of proteins may not represent promising targets for cancer therapy because there are many growth factors that can provide redundant growth-promoting signals; thus, when a sole factor is neutralized, other ligands or pathways may compensate [19]. However, in this study, we found that EREG was expressed at low levels in normal tissues, but exhibited high expression in 9 of 11 human carcinoma cell lines (Supplementary Fig. 2), suggesting a role for EREG in cancer progression. Kobayshi and colleagues recently reported that anti-EREG antibodies may be efficacious in the early stages of cancer development, when cancers have high levels of cancer stem cells [20]. These data indicated that anti-EREG antibodies may be an effective anticancer therapy and could be expected to exert synergistic anticancer activities with traditional chemotherapeutic agents, such as irinotecan, in the treatment of colorectal cancer.

In the present study, the initial version of the humanized antibody (HM0) was constructed by simply grafting CDRs from the 9E5 light or heavy chain to the human antibody light or heavy chain. Antigen-binding activity assays indicated that this version lost EREG binding activity. Grafting of the CDRs of murine antibodies onto appropriate human frameworks, a more common method, has often resulted in reduced affinity or activity for the target antigen [21]. Because the CDR-grafting method is widely used for humanizing murine antibodies, there are only a few general strategies for recovering the binding affinity of humanized antibodies, and these strategies often require several trial-and-error approaches [22]. In this study, a reliable 3D model of the variable regions of the 9E5 antibody was built using computer-aided homology modeling. We focused on the L49 residue and FR resides of the CDR-L2 loops because the residues of the mutation-induced conformations differed from those of the mature mAb. The mutation could influence the stabilization of the 9E5 variable region and the conformation of the CDRs and the β-sheet, which fix the structure of the CDR loops (Supplementary Fig. 1A). For other FR resides, the expected conformational rearrangement of the CDR loop region was not observed. Indeed, L49H was relatively exposed and in direct contact with the antigen; 2ADF and 1FJ1, for example, were 98% and 90% identical with 9E5, respectively (Supplementary Fig. 1B and C). This result may not be expected after database searches since VL residue 49 is usually a tyrosine in human and murine germline VL genes (Supplementary Fig. 1D). Consequently, back-mutation of the L49 residue (tyrosine to histidine) led to generation of HM1, which completely restored the binding affinity of its murine counterpart. Importantly, this HM1 antibody bound to EREG and efficiently mediated ADCC in DLD-1 and HCT116 colorectal cancer cells, which overexpress EREG, as anticipated by its human IgG1 constant region. The human IgG1 constant region was employed primarily because of its capacity to induce human effector functions, such as ADCC. In contrast, the murine parent antibody 9E5 was not very effective in mediating ADCC in either DLD-1 or HCT116 cells.

In conclusion, our results demonstrated that HM1 generated by this approach retained antigen binding affinity and activity similar to its parental counterpart. Given that HM1 has targeted cytotoxicity and is expected to have lower immunogenicity through resurfacing the variable region and human IgG1 constant region, we predict that HM1 may have potential applications in the clinical diagnosis and treatment of patients with EREG-positive cancers.

Acknowledgments

This work was supported in part by Creation of Innovation Centers for Advanced Interdiciplinary Research Areas Program, Ministry of Education, Culture, Sports, Science and Technology-Japan.

Appendix A. Supplementary data

Supplementary data associated with this article can be found, in the online version, at http://dx.doi.org/10.1016/j.bbrc.2013.11.014.

References

[1] Y. Yarden, M.X. Sliwkowski, Untangling the ErbB signalling network, Nat. Rev. Mol. Cell Biol. 2 (2001) 127–137.
[2] O.M. Fischer, S. Hart, A. Gschwind, et al., EGFR signal transactivation in cancer cells, Biochem. Soc. Trans. 31 (2003) 1203–1208.
[3] D.S. Salomon, R. Brandt, F. Ciardiello, et al., Epidermal growth factor-related peptides and their receptors in human malignancies, Crit. Rev. Oncol. Hematol. 19 (1995) 183–232.
[4] H. Toyoda, T. Komurasaki, D. Uchida, et al., Epiregulin A novel epidermal growth factor with mitogenic activity for rat primary hepatocytes, J. Biol. Chem. 270 (1995) 7495–7500.
[5] S. Shirasawa, S. Sugiyama, I. Baba, et al., Dermatitis due to epiregulin deficiency and a critical role of epiregulin in immune-related responses of keratinocyte and macrophage, Proc. Natl. Acad. Sci. USA 101 (2004) 13921–13926.
[6] I. Baba, S. Shirasawa, R. Iwamoto, et al., Involvement of deregulated epiregulin expression in tumorigenesis *in vivo* through activated Ki-Ras signaling pathway in human colon cancer cells, Cancer Res. 60 (2000) 6886–6889.
[7] F. Revillion, V. Lhotellier, L. Hornez, et al., ErbB/HER ligands in human breast cancer, and relationships with their receptors, the bio-pathological features and prognosis, Ann. Oncol. 19 (2007) 73–80.
[8] N. Tørring, F.D. Hansen, B.S. Sørensen, et al., Increase in amphiregulin and epiregulin in prostate cancer xenograft after androgen deprivation-impact of specific HER1 inhibition, Prostate 64 (2005) 1–8.
[9] S. Freimann, I. Ben-Ami, L. Hirsh, et al., Drug development for ovarian hyperstimulation and anti-cancer treatment: blocking of gonadotropin signaling for epiregulin and amphiregulin biosynthesis, Biochem. Pharmacol. 68 (2004) 989–996.
[10] P. Carter, Improving the efficacy of antibody-based cancer therapies, Nat. Rev. Cancer 1 (2001) 118–129.
[11] M.-P. Lefranc, IMGT-ontology and IMGT databases, tools and Web resources for immunogenetics and immunoinformatics, Mol. Immunol. 40 (2004) 647–660.
[12] C. Chothia, A.M. Lesk, E. Gherardi, et al., Structural repertoire of the human VH segments, J. Mol. Biol. 227 (1992) 799–817.
[13] A. Sircar, E.T. Kim, J.J. Gray, Rosetta antibody: antibody variable region homology modeling server, Nucleic Acids Res. 37 (2009) W474–W479.
[14] E.F. Pettersen, T.D. Goddard, C.C. Huang, et al., UCSF Chimera-A visualization system for exploratory research and analysis, J. Comput. Chem. 25 (2004) 1605–1612.
[15] J.T. Pedersen, A.H. Henry, S.J. Searle, et al., Comparison of surface accessible residues in human and murine immunoglobulin Fv domains. Implication for humanization of murine antibodies, J. Mol. Biol. 235 (1994) 959–973.

[16] R. Sasada, H. Onda, K. Igarashi, The establishment of IL-2 producing cells by genetic engineering, Cell Struct. Funct. 12 (1987) 205.
[17] A. Sivasubramanian, A. Sircar, S. Chaudhury, et al., Toward high-resolution homology modeling of antibody Fv regions and application to antibody-antigen docking, Proteins 74 (2009) 497–514.
[18] H.H. Trutnau, New multi-step kinetics using common affinity biosensors saves time and sample at full access to kinetics and concentration, J. Biotechnol. 124 (2006) 191–195.
[19] R. Harris, EGF receptor ligands, Exp. Cell Res. 284 (2003) 2–13.
[20] S. Kobayashi, H. Yamada-Okabe, M. Suzuki, et al., LGR5-positive colon cancer stem cells interconvert with drug-resistant LGR5-negative cells and are capable of tumor reconstitution, Stem Cells 30 (2012) 2631–2644.
[21] P.T. Jones, P.H. Dear, J. Foote, et al., Replacing the complementarity-determining regions in a human antibody with those from a mouse, Nature 321 (1986) 522–525.
[22] H. Gram, L.A. Marconi, C.F. Barbas, et al., In vitro selection and affinity maturation of antibodies from a naive combinatorial immunoglobulin library, Proc. Natl. Acad. Sci. USA 89 (1992) 3576–3580.